ADVANCED MATERIALS
www.advmat.de

Fully Degradable Protein Gels with Superior Mechanical Properties and Durability: Regulation of Hydrogen Bond Donors

Yunfeng Li, Zhihui Qin, Ping He, Muqing Si, Linfang Zhu, Na Li, Xiaojiao Shi, Guanqiu Hao, Tifeng Jiao,* and Ximin He**

Protein gels hold great promise in various applications due to their high biocompatibility, biodegradability, and abundant sources. However, most existing protein gels suffer from low strength, stiffness, and toughness because conventional solvent within gels usually weakens crosslinked network structure. Here, strong, stiff, and tough protein gels are developed by using deep eutectic solvents (DESs) with tunable hydrogen bond donors (HBDs) as the dispersion medium. The DESs not only facilitate protein chain–chain interaction, but also form abundant non-covalent crosslinks between protein chains through protein chain–solvent interaction. More importantly, these crosslinked interactions can be tailored by varying HBDs, further toughening the gels. As a result, the obtained protein gels exhibit excellent mechanical properties, including tensile strength of 10.25 ± 1.28 MPa, tensile strain of $892.51 \pm 39.66\%$, elastic modulus of 24.57 ± 0.27 MPa, toughness of 17.34 ± 0.46 MJ m^{-3}, and fracture energy of 6.76 ± 0.99 kJ m^{-2}, which surpass the previously reported protein gels. Despite their enhanced mechanics, they retain key advantages such as adhesiveness, retrievability, environmental durability, and full degradability. This work presents a novel strategy for designing robust, multifunctional protein gels, expanding their potential in emerging technologies that demand both mechanical toughness and functional versatility.

1. Introduction

Protein-based gels, as biomimetic soft-wet materials composed of solvents embedded within three-dimensional polymer network, have attracted considerable attention due to their intrinsic advantages including high biocompatibility, regulable degradability, sustainability, as well as multiple reactive sites for functionalization.[1–3] These features make them promising candidates for applications in diverse applications such as tissue engineering,[4,5] flexible electronics,[6,7] and soft robotics.[8,9] However, most protein gels are derived from unstructured proteins and suffer from weak mechanical performance—characterized by low stiff, insufficient strength, and poor toughness, owing to the loosely organized and single crosslinking network.[10,11] This seriously hinders their applicability in load-bearing materials, which usually requires the ability to withstand repetitive and large mechanical forces under complex conditions. Additionally, in many cases, protein gels also need to have further properties, such as environmental stability (anti-freezing), fracture resistance and adhesiveness, to perform effectively under critical conditions. Therefore, the development of mechanically robust, stiff, tough, and multifunctional protein-based gels is greatly imperative.

Leveraging the abundant functional groups in proteins that serve as non-covalent bonding sites, significant efforts have been made to strengthen and toughen protein gels by regulating non-covalent associations between protein chains, including hydrophobic aggregation,[12,13] ionic bonds,[14] and hydrogen bonds.[15,16] For example, Zhao et al. utilized $ZnSO_4$ solution to induce metal coordination and hydrophobic interactions in covalently crosslinked elastin-like polypeptides, resulting in a tough protein gel with tensile strength of 2.5 MPa.[17] Similarly, our previous work reported a gelatin protein gel with improved tensile strength (3.0 MPa) by soaking gelatin hydrogel into a sodium citrate (Na_3Cit) water/glycerol solution to induce hydrophobic aggregation, hydrogen bond and ionic crosslinking of gelatin chains.[18] Comparable strategies have been applied to

Y. Li, Z. Qin, L. Zhu, N. Li, X. Shi, T. Jiao
State Key Laboratory of Metastable Materials Science and Technology
Hebei Key Laboratory of Applied Chemistry
Hebei Key Laboratory of Nanobiotechnology
Yanshan University
Qinhuangdao 066004, China
E-mail: zhqin@ysu.edu.cn; tfjiao@ysu.edu.cn
Z. Qin, G. Hao
Department of Chemical and Biomolecular Engineering
National University of Singapore
4 Engineering Drive 4, Singapore 117585, Singapore
P. He, M. Si, X. He
Department of Materials Science and Engineering
University of California
Los Angeles, CA 90095, USA
E-mail: ximinhe@ucla.edu

The ORCID identification number(s) for the author(s) of this article can be found under https://doi.org/10.1002/adma.202506577

DOI: 10.1002/adma.202506577

facilitate the non-covalent crosslinking of gelatin chains, improving the mechanical performance.[19–21] However, these reported protein gels exhibited limited mechanical improvements (elastic modulus < 0.5 MPa, tensile strength < 5 MPa, fracture energy < 1 kJ m^{-2}). In fact, current research on toughening protein gels mainly focuses on regulating interactions between protein chains to dissipate energy or distribute stress in gel networks during deformation.[22,23] Solvents, as the dispersion medium occupying a large part (usually >50 wt%) of gels, are generally ignored or regarded as a factor that deteriorates the mechanics of the gels by blocking protein chain–chain interactions.[24] Solvent molecules (e.g., water, DMSO) are typically small with few functional groups, allowing them to bond with only one protein chain rather than bridging multiple chains. As a result, protein chain–solvent interaction distances the protein chains and weaken the network, and the limited number of crosslinking points within gel networks makes it difficult to obtain protein gels that simultaneously exhibit high stiffness, strength, and toughness. As solvents constitute the majority of protein gels, if solvent molecules could bridge different protein chains through forming protein chain–solvent interaction, the mechanical performance could be significantly enhanced.

Deep eutectic solvents (DESs) are a class of liquid-state mixture of hydrogen bond acceptors (HBAs, e.g., quaternary ammonium salts) and hydrogen bond donors (HBDs, e.g., amide, carboxylic acid, or polyol) formed under strong hydrogen bonding and electrostatic forces between two components. DESs possess the merits of low vapor pressure, low freezing point, good conductivity, and non-toxicity.[25,26] Particularly, in DESs containing polyol-based HBDs, abundant hydroxyl groups offer multiple bonding sites to form hydrogen bonds with functional groups (such as –OH, –O, $–NH_2$) present in protein chains. Therefore, DESs are emerging as a promising medium for constructing gels (denoted as eutectogels) with high stability and environment-tolerance. Recently, protein gels with high ductility and good anti-freezing performances have been prepared by directly introducing DESs into protein network.[27–29] However, these works are mainly focused on utilizing DESs as solvent to improve stability of the gels or exploiting weak compatibility of DESs with protein to increase interactions between protein chains to strengthen the resulted gels. The presence of abundant solvents, which was not utilized as effective crosslinking for protein chains, leading to a loosely crosslinked network. As a result, the reported protein gels with DESs as solvent rarely achieved a combination of high stiffness, strength, and toughness. Thus, we hypothesize that the DESs can induce the enhancement of interactions between protein chains while multiple hydroxyl groups in DESs can form hydrogen bonds with functional groups on different protein chains to bridge protein chains by the reasonable regulation and optimization of components, achieving simultaneous enhancement in protein chain-chain and protein chain–solvent interactions for strengthening and toughening the gel.

Here, we demonstrate the synergy effect of the enhanced protein chain–chain and protein chain–solvent interactions by using DESs with tunable HBDs as solvent to regulate and crosslink protein chains for greatly improving the mechanical performance of protein gels. Following this design concept, we report the fabrication of a robust, stiff and tough protein gel based on low-cost and easy-operated gelatin protein. In our system, the DESs not only strengthen the gelatin chain–chain interactions, but also form abundant and strong noncovalent crosslinks between gelatin chains at optimized concentration. In particular, HBDs with varying number of hydroxyl groups effectively modulate hydrogen bonds between DESs and gelatin chains, further toughening mechanics of the gel. The obtained protein gels (named as gelatin eutectogels) possess high strength, stiffness and toughness, and insensitivity to crack propagation. Moreover, these gels also exhibit excellent anti-freezing ability, adhesiveness and recyclability, as well as full degradability. Such multifunctional, strong and tough protein gel holds great potential in cutting-edge applications including artificial tissues, soft robotics, and stretchable electronics.

2. Results and Discussion

2.1. Fabrication of Strong, Stiff, and Tough Gelatin Eutectogels

A series of DESs with different HBDs were used to regulate protein chain–chain and chain–solvent interactions for simultaneously strengthening and toughening protein gels. Choline chloride (ChCl) was chosen as the HBA due to its natural origin, excellent biocompatibility, low toxicity, and its ability to form DESs with various polyols.[25] These DESs were synthesized by mixing ChCl with polyols, respectively ethylene glycol (EG), glycerol (Gly), xylitol, and D-sorbitol, under continuous stirring at 60 °C to give a uniform solution (Figure S1, Supporting Information), which were named as ChCl-EG, ChCl-Gly, ChCl-Xylitol, or ChCl-(D-Sorbitol), respectively. The polyols served as HBDs to associate with ChCl (HBA) via strong hydrogen bonds or ion–dipole interactions. For example, the chemical structure and interactions of ChCl-Gly were characterized by Fourier transform infrared (FT-IR) spectra (Figure S2, Supporting Information). The –OH characteristic peak in ChCl-Gly shifted to 3310 cm^{-1} and became broader compared to that of Gly (3297 cm^{-1}) and ChCl (3217 cm^{-1}) due to hydrogen bonds and ion–dipole interactions.[30] Then, gelatin protein was selected, and the obtained DESs were utilized to fabricate strong and tough protein gels according to the procedures illustrated in **Figure 1a**. First, gelatin powder was fully dissolved in deionized water followed by cooling at 4 °C to obtain gelatin hydrogel, where gelatin chain was crosslinked by forming interchain triple helixes. Next, a protein gel, referred to as gelatin eutectogel, was obtained by soaking gelatin hydrogel in DESs for 24 h to replace the water. Solvent replacement promoted the non-covalent interactions between gelatin chains such as hydrogen bonds and ionic interactions. Meanwhile, DES molecules were bonded to polymer chains and served as interchain molecular bridges to crosslink the polymer network. The synergy between multiple crosslinking structures of gelatin chain–chain and chain–DESs (such as hydrogen bonding and ionic interactions) led to form strong and tough gelatin eutectogels. As shown in the Figure 1b,c, the highly transparent $gelatin_{15}$/ChCl-Gly (G_{15}/ChCl-Gly) gel (where the 15 referred to the initial gelatin mass fraction) could lift 500 g weight, which was ≈1500 times of its own weight. Notably, such tunable non-covalent crosslinked network and DESs endowed these gelatin eutectogels with multiple desirable performances including high toughness, high stiffness, high strength, superior

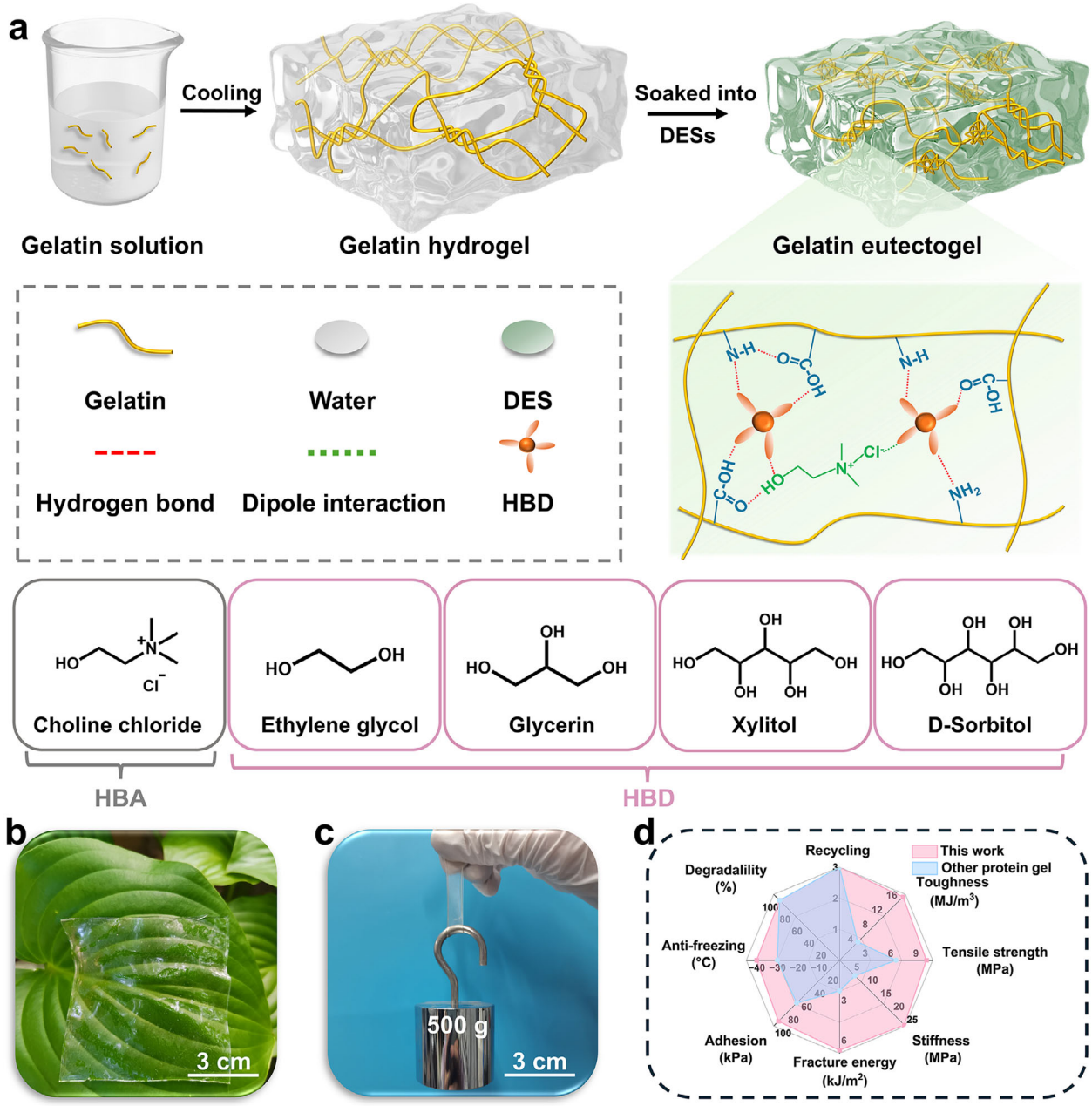

Figure 1. Fabrication and non-covalent interaction mechanism of protein gel (gelatin eutectogel). a) Schematics of preparation process and hydrogen bond donor (HBD) regulation mechanism of gelatin eutectogel. Four types of DESs with same hydrogen bond acceptor (HBA, ChCl) and different HBDs (EG, Gly, xylitol, D-Sorbitol). b) Transparency of G_{15}/ChCl-Gly gel. c) Illustration of the high strength of G_{15}/ChCl-Gly gel (50 mm × 10 mm × 0.65 mm) by withstanding a 500 g weight. d) Versatility of gelatin eutectogel (toughness, strength, stiffness, fracture resistance, adhesion, recycling, anti-freezing and degradability).

fracture resistance, adhesion, recycling, anti-freezing ability and degradability (Figure 1d, Table S1, Supporting Information).

2.2. Characterization and Molecular Mechanism of Gelatin Eutectogels

To reveal the tunable crosslinked interactions and structural evolution of the gelatin eutectogels, a series of characterizations were performed. Taking G_{15}/ChCl-Gly gel as an example, thermogravimetric analysis (TGA) demonstrated that after 24 h of solvent replacement, free water was completely removed, leaving only a small amount of bound water (Figure S3, Supporting Information). As revealed by scanning electron microscopy (SEM) and the corresponding energy-dispersive spectroscopy (EDS) mapping images (**Figures** 2a, and S4, Supporting Information), compared with the loose porous structure and even C, N, O elements distribution on gel skeleton of gelatin hydrogel, the obtained

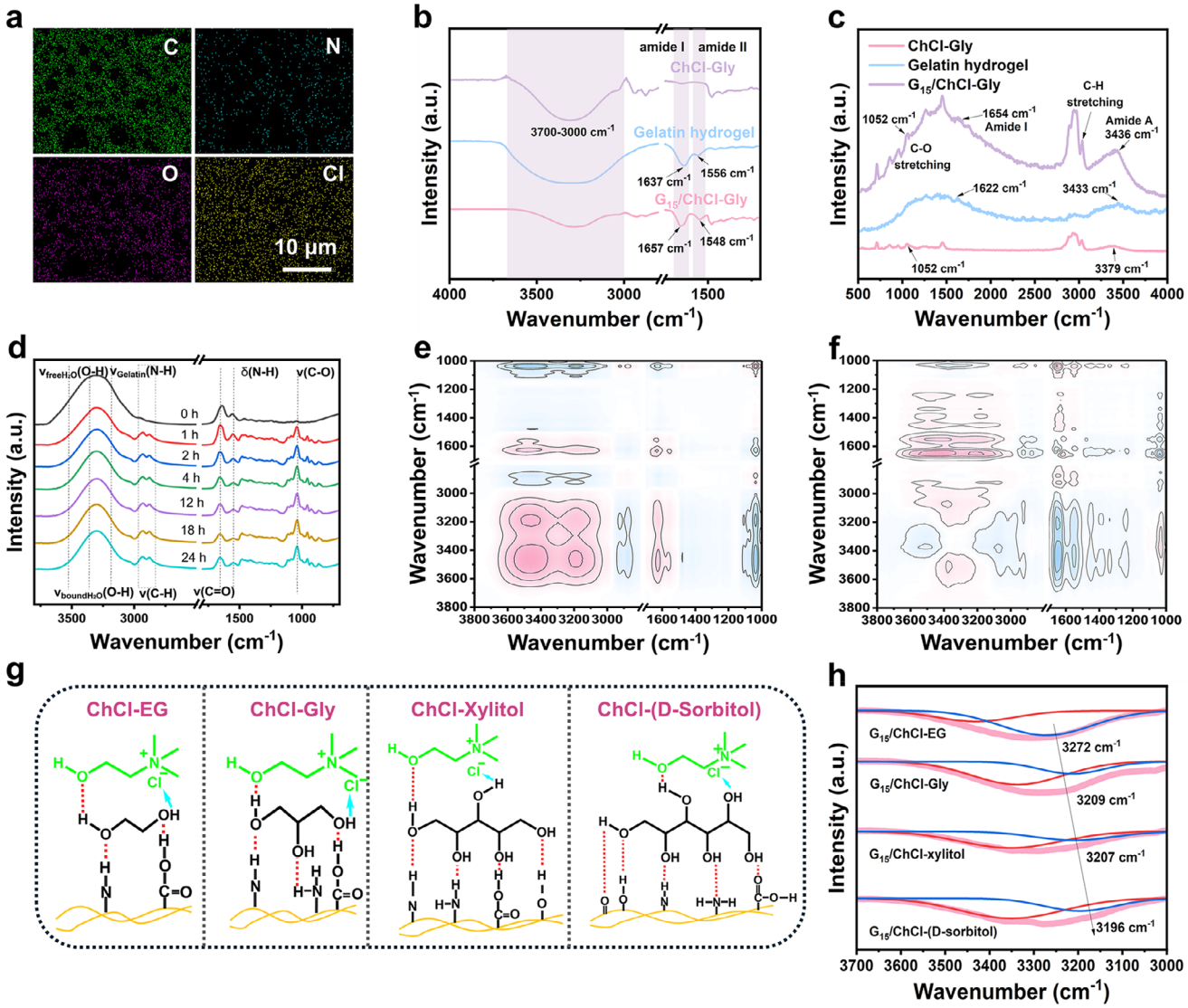

Figure 2. Characterization of gelatin eutectogels. a) EDS mapping images of G_{15}/ChCl-Gly gel. b) FTIR spectra and c) Raman spectra of ChCl-Gly, gelatin hydrogel and G_{15}/ChCl-Gly gel. d) FT-IR spectra of G_{15}/ChCl-Gly gel during solvent replacement at different soaking times (1, 2, 4, 12, 18, and 24 h). e) 2DCOS synchronous and f) asynchronous spectra generated from (d). In 2DCOS spectra, the red areas represent positive correlation intensity, while blue areas represent the negative correlation intensity. g) Hydrogen bond interactions between HBDs in different DESs (ChCl-EG, ChCl-Gly, ChCl-Xylitol, ChCl-(D-Sorbitol)) and gelatin chains. h) FT-IR spectra and the peak fitting curves of different gelatin eutectogels (G_{15}/ChCl-EG, G_{15}/ChCl-Gly, G_{15}/ChCl-Xylitol, G_{15}/ChCl-(D-Sorbitol)).

G_{15}/ChCl-Gly gel exhibited the denser porous structure, and except for the uniform distribution of C, N, O on gel skeleton, which are present in both gelatin and DES, the Cl from the DES was uniformly distributed within G_{15}/ChCl-Gly gel. These results suggest that the solvent molecules were intercalated between gelatin chains and prompted the formation of dense and uniform structure of G_{15}/ChCl-Gly gel. FT-IR spectroscopy was conducted to identify interactions inside G_{15}/ChCl-Gly gel (Figure 2b). The gelatin hydrogel exhibited a characteristic peak of amide I located at 1635 cm^{-1}, which is correlated to C = O stretching vibrations of the peptide linkages, and a characteristic peak of amide II at 1556 cm^{-1}, which is associated with N–H bending. The shift and change of amide I and II bands are usually correlated to the change of interactions between gelatin chains.[31,32] After replacing water with ChCl-Gly, the peak of amide I blue-shifted to 1647 cm^{-1}, and the peak of amide II red-shifted to 1548 cm^{-1} in G_{15}/ChCl-Gly gel, indicating the enhanced crosslinked interactions between gelatin chains (such as hydrogen bonds and ionic interactions) by the addition of DES. Besides, there was a broad peak in the range of 3000–3700 cm^{-1} in G_{15}/ChCl-Gly gel, belonging to the stretching vibration of O–H and N–H. A peak fitting method was performed on the absorption peak in the range of 3000–3700 cm^{-1} (Figure S5, Supporting Information). The O–H stretching vibration peak of Gly in G_{15}/ChCl-Gly gel shifted from 3379 to 3336 cm^{-1} compared to that of ChCl-Gly.[33] And the peak at 3212 cm^{-1} ascribed to the N–H

stretching vibration in the spectrum of gelatin hydrogel shifted to 3209 cm^{-1} in the spectrum of G_{15}/ChCl-Gly gel.[34] These results evidence that the ChCl-Gly was introduced and the formed hydrogen bonds with gelatin chains. The hydrogen bonds of ChCl-Gly and gelatin chains can also be confirmed by ^{1}H-NMR (Figure S6, Supporting Information), where the characteristic peak of the active hydrogen (hydroxyl groups at terminal positions of glycerol) at 4.62 ppm in ChCl-Gly moved toward 4.61 ppm in G_{15}/ChCl-Gly gel and the characteristic peak at 7.95 ppm, corresponding to the active hydrogen (the amide group) of glycine in gelatin chain, shifted to 8.36 ppm in G_{15}/ChCl-Gly gel.[35,36] The interaction between gelatin and ChCl-Gly was further verified by Raman characterization. As shown in Figure 2c, G_{15}/ChCl-Gly gel had obvious C–O and C–H stretching peaks, which were due to the increase of hydroxyl groups and alkyl groups with the addition of ChCl-Gly. The peak of amide A corresponding to the stretching vibrations of N–H and O–H widened and blue-shifted, indicating an increase in the number of intramolecular and intermolecular hydrogen bonds among gelation chains and ChCl-Gly.[21,37] In addition, the absorption peak of amide I slightly shifted to higher wavenumbers, also evidencing the increase of interactions between gelatin chains. Moreover, wide-angle X-ray scattering (WAXS) was conducted to investigate the influence of the introduction of DES on chain conformation of gelatin. As shown in Figure S7, Supporting Information, different from the gelatin hydrogel with two distinct diffraction peaks located at 8.5° (corresponding to the diameter of the triple helix perpendicular to the chain direction) and 30.4° (corresponding to the distance between proline in the turns of the polyproline-II-helix single helix), the G_{15}/ChCl-Gly gel only exhibited a prominent diffraction peak at 19.4° corresponding to the locally ordered arrangements of the random coiled polypeptide chains formed by hydrogen bonds,[38,39] which may be attributed to the enhanced interactions between the random coiled chains and the inhibiting effect of choline chloride in triple helix structures, making the triple-helix structure less distinct. In summary, the introduction of ChCl-Gly reinforced hydrogen bonding of unordered gelatin chains and formed additional crosslinking sites with gelatin chains.

Subsequently, for getting deeper insights into the formation process of gelatin eutectogels, the weight changes and FT-IR spectra of G_{15}/ChCl-Gly gels in different soaking times were conducted. As shown in Figure S8, Supporting Information, when the soaking time increased from 0 to 24 h (with the DESs replaced once after 18 h), both the weight and size of the gels gradually decreased. Particularly, the weight of gels exhibited sharp decrease as the soaking time increased within 4 h. These results indicate that the rapid solvent diffusion outward occurred in the gelatin gel, which strengthened the non-covalent interactions between protein chains inside the gels. However, when the soaking time further increased to 36 h, the weight of the gels slightly increased, which maybe attribute to the entrance of more ChCl-Gly into the gel. FT-IR spectra of G_{15}/ChCl-Gly with various soaking times (1, 2, 4, 12, 18, and 24 h) were recorded, as shown in Figure 2d. The O–H stretching vibrations of free water, bound water, and Gly were located at 3589, 3452, and 3336 cm^{-1}, respectively. The N–H stretching vibration (ν (N–H)) in the gelatin chain was observed at 3215 cm^{-1}. The peaks at 2980, 2880, and 1030 cm^{-1} corresponded to the C–H asymmetrical (ν_{as}(C–H)) and symmetrical (ν_s(C–H)) stretching vibration of $–CH_3$, and the stretching vibration (ν(C–O)) of C–OH in DESs, respectively. And the peaks at 1635 and 1524 cm^{-1} corresponded to the stretching vibration of C = O (ν (C = O)) and the bending vibration of N–H (δ (N–H)) of gelatin chains, respectively.[40,41] As the soaking time increased, the ν (O–H) peaks red-shifted and decreased, while the peaks of the ν_{as}(C–H), ν_s(C–H), and ν(C–O) increased, and the peaks of the amide region blued-shifted and decreased. Such transition originated from the enhanced crosslinked interactions inside the gelatin gel owing to both the dehydration and simultaneous increasement of deep eutectic solvent within the gels. Two-dimensional correlation spectroscopy (2DCOS) was applied to further extract more subtle information of the hydrogel-to-eutectogel transition during the soaking process. Synchronous and asynchronous 2DCOSY spectra were calculated from time-correlated FT-IR spectra (Figure 2e,f). According to Noda's judgment rule,[42,43] the response order of different functional groups to the soaking time was determined as: 2930 cm^{-1}→2860 cm^{-1} → 3336 cm^{-1} →3452 cm^{-1} → 3215 cm^{-1} → 3589 cm^{-1} → 1030 cm^{-1} → 1635 cm^{-1}→ 1524 cm^{-1}, that was, ν_{as}(C–H) → ν_s(C–H) → ν(O–H) → $\nu_{bound\ water}$(O–H) → ν(N–H) → $\nu_{free\ water}$(O–H) → ν(C–O) → ν(C = O) → δ (N–H).

From the combination of weight change and FT-IR analysis, the formation process of gelatin eutectogel can be described as follows: When the gelatin hydrogel was soaked in DESs, the water molecules in the hydrogel quickly diffused to DESs, while the DESs simultaneously diffused into the gel, which induced the transformation of bound water to free water in the gels due to the strong binding of DESs to water, with the free water then diffusing out into the environment. The diffusion rate of water into the environment was greater than that of the DESs into the gel, leading to dehydration. This process resulted in the enhancement of the interactions between gelatin chains and the formation of hydrogen bonds between DESs and gelatin chains driven by the solvent diffusion dynamics.

The HBDs in DESs can build hydrogen bonding with gelatin chains, providing the effective crosslinking points to increase the crosslinking density of the eutectogels. Owing to the adjustability of HBDs in DESs, the crosslinked interactions between DESs and gelatin chains in eutectogels were regulated by changing the HBDs (EG, Gly, xylitol, D-sorbitol) of DESs (Figure 2g). Specifically, as the number of hydroxyl groups in HBDs from EG, Gly, and xylitol to D-sorbitol increased, one HBD provided more hydrogen bond sites, which allowed for more hydrogen bonding with gelatin chains. More importantly, polyhydroxyl HBDs had more chances to interact with various gelatin chains, thus forming effective cross-linking points. The actual composition of different gelatin eutectogels (G_{15}/ChCl-EG, G_{15}/ChCl-Gly, G_{15}/ChCl-Xylitol, and G_{15}/ChCl-(D-Sorbitol)) were conducted and calculated based on the weighing and thermogravimetric experiments (Figure S9, Supporting Information). The results show that the actual gelatin content increased when the number of hydroxyl groups in HBDs increased, which indicates the formation of the denser crosslinked structures, impeding the entrance of more DESs into the gel. The changes of crosslinked structure between gelatin and different DESs were identified by FT-IR spectra (Figure 2h and Figure S10, Supporting Information). After the replacement with various DESs, all gelatin eutectogels exhibited a broad peak in the range of 3000–3700 cm^{-1}, corresponding to the stretching vibration of O–H

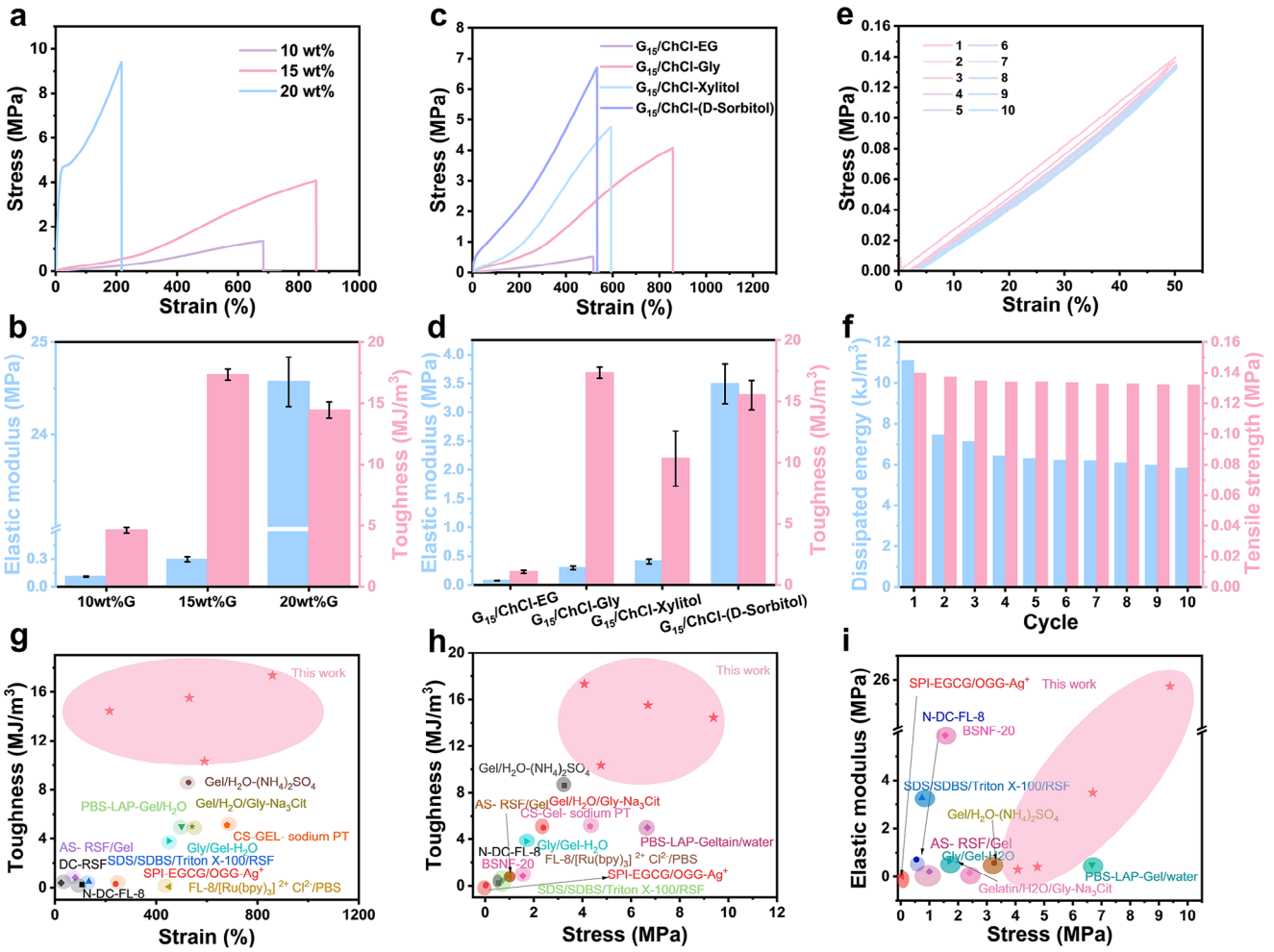

Figure 3. Tunable mechanical properties of gelatin eutectogels. a) Typical tensile stress-strain curves and b) the corresponding elastic modulus and toughness of G/ChCl-Gly gel with different gelatin content (10, 15, and 20 wt%). c) Typical tensile stress–strain curves and d) the corresponding elastic modulus and toughness of gelatin eutectogels prepared by DESs with different HBDs (G_{15}/ChCl-EG, G_{15}/ChCl-Gly, G_{15}/ChCl-Xylitol, G_{15}/ChCl-(D-Sorbitol)). e) Ten successive cyclic tensile loading–unloading curves and f) the corresponding dissipated energy and tensile strength of G_{15}/ChCl-Gly gel. Comparison between the prepared gelatin gels and the reported representative protein gels: g) toughness in relation to tensile strain, h) toughness in relation to tensile stress, and i) elastic modulus in relation to tensile stress. Data in (b) and (d) are represented as mean values ± SD ($n = 3$).

and N–H. A peak fitting method was conducted in the range of 3000–3700 cm^{-1}, where the peak of N–H stretching vibration was located at 3272–3196 cm^{-1}. With the increase in the number of hydroxyl groups in HBDs, the corresponding position of N–H stretching vibration in gelatin chains shifted from 3272 to 3196 cm^{-1}, suggesting that stronger hydrogen bonds were formed in gelatin eutectogels containing more hydroxyl HBDs.[34] The characteristic peaks associated with amide regions of gelatin were nearly similar for all gelatin eutectogels. In addition, the chain conformation of the different gelatin eutectogels was investigated by WAXS (Figure S11, Supporting Information). It can be seen that the distinct diffraction peak associated with the locally ordered arrangements of the random coiled chains gradually moved to a smaller angle with the increase of the number of hydroxyl groups in HBDs, showing solvents or small molecules can be inserted between polymer chains to form hydrogen bonds and occupy space.[44] These results further indicate that hydrogen bonding between DESs and gelatin chains can be regulated by changing HBDs, thus contributing to the tunable mechanical performance.

2.3. Mechanical Performances of Gelatin Eutectogels

The facile introduction of DESs densifies the network structure by facilitating the interactions between gelatin chains and forming hydrogen bonds with gelatin chains, inducing the great improvement of mechanical properties of gelatin eutectogels, which were then systematically investigated. First, a series of G/ChCl-Gly gels with various initial gelatin content were prepared to regulate the mechanical properties (**Figure 3a,b**). The G_{10}/ChCl-Gly gel with gelatin content of 10 wt% has tensile strength of 1.33 ± 0.08 MPa and elastic modulus of 0.11 ± 0.005 MPa. As elevating gelatin content from 10 to 20 wt%, the G_{20}/ChCl-Gly gel was greatly strengthened, with the tensile strength and elastic modulus increased to 10.25 ± 1.28 and 24.57 ± 0.27 MPa,

respectively. Meanwhile, the G/ChCl-Gly gel was also significantly toughened, with the maximum toughness of 17.34 ± 0.46 MJ m^{-3} when gelatin content was 15 wt%. However, further increasing gelatin content would stiffen the gels at the sacrifice of stretchability, reducing toughness. These results demonstrate that by modulating the gelatin content, the G/ChCl-Gly gels exhibit a wide mechanical tunability, ranging from soft and extensible to tough and highly stretchable, or even stiff and robust. Especially, the tensile strength, elastic modulus and toughness of G_{20}/ChCl-Gly gel were 2564%, 61 429%, and 11 230% higher than those of gelatin hydrogel, respectively (Figure S12, Supporting Information). Apparently, the significant change in mechanical properties cannot be solely attributed to increasing strand density. Instead, it results from the synergistic effect of gelatin chain–chain and chain–solvent interactions. The DES (ChCl-Gly) can not only induce non-covalent interactions of gelatin chains but also act as crosslinkers to bridge gelatin chains by hydrogen bonds, which was verified by FT-IR, ^{1}H NMR and Raman characterizations (Figure 2a,b and Figure S6, Supporting Information). The actual gelatin contents in G_{10}/ChCl-Gly, G_{15}/ChCl-Gly and G_{20}/ChCl-Gly gels were measured to 24.30, 32.63, and 43.46 wt%, respectively (Figure S13, Supporting Information). Small-angle X-ray scattering (SAXS) revealed that the interchain distance of gelatin chains of G_{10}/ChCl-Gly, G_{15}/ChCl-Gly, G_{20}/ChCl-Gly gels were 1.817, 1.807 and 1.726 nm, respectively (Figure S14, Supporting Information).[45,46] At low gelatin content (low polymer-to-DES ratio), the density of polymer chains was low and the distance between the chains was large. Thus, there were fewer crosslinking points between gelatin chains, resulting in softness and low strength. As the gelatin content increased, the density of polymer chains increased, while the distance between the chains decreased. The gelatin chain–chain interactions increased, and more crosslinking points between gelatin chains bridged by DES formed, thus improving stiffness, tensile strength and toughness. When the gelatin content further increased, the shortening of interchain distance enabled the abundant DES-mediated hydrogen bonds to crosslink gelatin chains, resulting in high stiffness and tensile strength. However, the excessively high cross-linking density at high gelatin content reduced the mobility of gelatin chain segments, decreasing the stretchability.[47] Thus, the toughness also exhibited a slight decrease.

The HBDs in DESs act as crosslinkers to bridge the polymer chains by hydrogen bonds, which can be regulated by different amount of hydroxyl groups of HBDs (EG, Gly, xylitol, and (D-sorbitol)) (Figure 2g,h). To study the influence of HBDs on the mechanical properties of gelatin eutectogels, four type of the gelatin eutectogels (G_{15}/ChCl-EG, G_{15}/ChCl-Xylitol, and G_{15}/ChCl-(D-Sorbitol)) were compared by tensile tests (Figure 3c,d). The mechanical performance of gelatin eutectogels was highly relevant with the composition of DES solvents. The G_{15}/ChCl-EG gel with two hydroxyl groups in HBD exhibited relatively weak mechanical properties (tensile strength of 0.53 ± 0.02 MPa, tensile strain of 544.00 ± 53.35%, elastic modulus of 0.073 ± 0.002 MPa, and toughness of 1.08 ± 0.12 MJ m^{-3}). As previously proven, due to the formation of more hydrogen bonding interactions between DESs and polymer chains with the increase of the number of hydroxyl groups in HBDs (Figure 2h), the gelatin eutectogels became stiffer as the functionality of HBDs increased (from G_{15}/ChCl-EG to G_{15}/ChCl-(D-sorbitol)). The G_{15}/ChCl-(D-sorbitol) gel exhibited increased tensile strength of 6.34 ± 0.76 MPa and elastic modulus of 3.49 ± 0.35 MPa, respectively, as well as maintaining high toughness of 15.51 ± 1.18 MJ m^{-3} and tensile strain of 499.00 ± 62.71%. Therefore, the introduction of DESs with various HBDs can greatly enhance mechanical properties of the prepared gelatin eutectogels by adjusting hydrogen bonds between DESs and gelatin chains.

Taken together, the mechanical performance of gelatin eutectogels could be simply customized over a wide range by changing HBDs in DESs and gelatin contents (Table S2, Supporting Information), including tensile strength from 0.53 ± 0.02 to 10.25 ± 1.28 MPa, elastic modulus from 0.073 ± 0.002 to 24.57 ± 0.27 MPa, tensile strain from 200.80 ± 44.88 to 892.51 ± 39.66%, and toughness from 1.08 ± 0.12 to 17.34 ± 0.46 MJ m^{-3}. The mechanical properties of these gelatin eutectogels (including tensile strength, tensile strain, elastic modulus, and toughness) were compared with the representative protein gels reported in recent works (Figure 3g–i, Table S3, Supporting Information).[1,8,17–21,48–56] It can be seen that these values, particularly tensile strength and elastic modulus, far surpassed the reported protein-based gels.

The non-covalent crosslinked interactions in gelatin eutectogels are able to reversibly dissociate and reform, providing effective energy dissipation and self-recovery capacity. Loading–unloading tensile tests were conducted to evaluate the energy dissipation, using G_{15}/ChCl-Gly gel as an example (Figure S15, Supporting Information). A successive loading–unloading test under different maximum strains shows that the hysteresis loops became more obvious and the corresponding dissipation energy rose sharply with the increase of maximum strain. These results indicate that at small strains, the gel exhibited elastic deformation, accompanied by the dissociation of a limited number of non-covalent interactions. As the strains increased, more non-covalent crosslinked interactions dissociated, enabling effective energy dissipation to toughen the gels. Furthermore, we conducted 10 consecutive loading–unloading tests at 50% strain (Figure 3e,f). Apparently, a distinct hysteresis loop can be observed in the first cycle, with the dissipated energy being 11.09 kJ m^{-3}, indicating the rapid dissociation of abundant sacrificial bonds during deformation. From the second to tenth cycles, the size of hysteresis loops and the corresponding dissipated energy exhibited only a slight decrease. And the tensile stress in tenth cycle (0.132 MPa) was about 94.38% of that in the first cycle (0.134 MPa). These results reveal the good structural stability of the crosslinked networks even when partial crosslinking points were broken, as well as the good self-recovery ability of G_{15}/ChCl-Gly gel.

Crack-resistance ability is the merit for materials to prevent external attack, extending their service life.[57] The unique crosslinked structure imparts exceptional toughness to gelatin eutectogels regarding tear and fracture energy. Trouser-tearing test was first performed to evaluate the toughness of gelatin eutectogels (Figure 4a,b and Figure S16, Supporting Information). As shown in **Figure 4a**, a trouser-shaped notched G_{15}/ChCl-Gly sample can be highly stretched with a large moving distance. The calculated tearing energies increased from 0.37 ± 0.09 kJ m^{-2} (G_{15}/ChCl-EG) to 3.94 ± 0.50 kJ m^{-2} (G_{15}/ChCl-(D-sorbitol), all

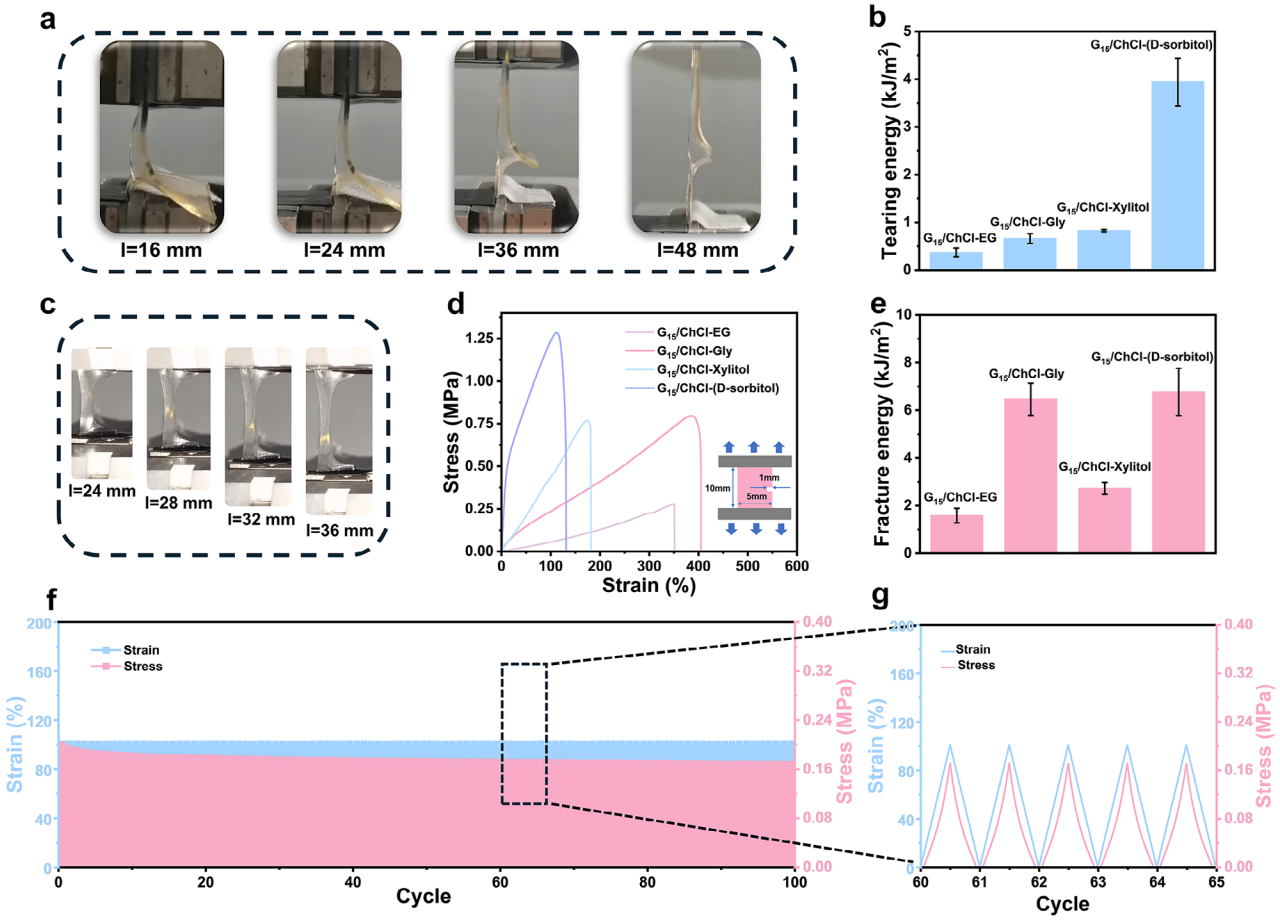

Figure 4. Insensitivity to crack propagation and fatigue resistance of gelatin eutectogels. a) Images of G_{15}/ChCl-Gly gel during tearing process. b) Tearing energies of different gelatin eutectogels ((G_{15}/ChCl-EG, G_{15}/ChCl-Gly, G_{15}/ChCl-Xylitol, G_{15}/ChCl-(D-Sorbitol)). c) Photographs of notched G_{15}/ChCl-Gly gel under stretching. d) Typical stress-strain curves and e) the corresponding fracture energy of the different notched eutectogels ((G_{15}/ChCl-EG, G_{15}/ChCl-Gly, G_{15}/ChCl-Xylitol, G_{15}/ChCl-(D-Sorbitol)). f) Consecutive tensile stress-strain curves of the notched G_{15}/ChCl-Gly gel at 100% strain for 100 cycles and g) magnified image showing no obvious stress attenuation. Data in (b) and (e) are represented as mean values ± SD ($n = 3$).

of which were higher than that of gelatin hydrogel (1.65 J m^{-2}) (Figure 4b and Figure S16, Supporting Information), demonstrating good tear tolerance. Furthermore, the fracture energy of gelatin eutectogels was evaluated by stretching single-edge notched samples (Figure 4c,e, Figure S17, Supporting Information). As shown in Figure 4c, when the notched G_{15}/ChCl-Gly sample was subjected to the loading perpendicular to the notched direction, it can be stretched to a large length without perceptible propagation of the crack tip,[58] indicating the excellent crack propagation insensitivity. Figure 4d shows that the notched samples of G_{15}/ChCl-EG, G_{15}/ChCl-Gly, G_{15}/ChCl-Xylitol, and G_{15}/ChCl-(D-Sorbitol) had large strains of 351%, 404%, 181%, and 131%, respectively. According to the crack propagation strains of notched samples and the stress–strain curves of unnotched samples, the calculated fracture energies of G_{15}/ChCl-EG, G_{15}/ChCl-Gly, G_{15}/ChCl-Xylitol, and G_{15}/ChCl-(D-Sorbitol) were 1.58 ± 0.31, 6.46 ± 0.67, 2.72 ± 0.25, and 6.76 ± 0.99 kJ m^{-2}, respectively. It should be noticed that the high fracture energies of G_{15}/ChCl-Gly and G_{15}/ChCl-(D-Sorbitol) gels can be attributed to the high toughness. Additionally, the fatigue-resistance capacity was evaluated by conducting continuous cyclic tensile tests on the notched G_{15}/ChCl-Gly gel at a fixed strain of 100% (Figure 4f,g). It is observed that the sample with a 1 mm notch exhibited negligible stress attenuation after 100 cycles at 100% strain, showing good fatigue resistance. The above results manifest that the dense structure, resulting from the synergistic interactions between abundant non-covalent gelatin chain–chain and chain–solvent interactions, effectively alleviates stress at the crack tip by dissociating some reversible bonds in the gelatin chains. This mechanism prevents crack propagation and contributes to the high crack resistance of the eutectogels. In summary, with such a large range of adjustable high mechanical properties (elastic modulus, tensile strength, and toughness) and mechanical durability, the gelatin eutectogels will be served as promising materials for wide applications of flexible sensors and biomimetic actuators in soft robotics.

2.4. Tough Gelatin Eutectogels with Multifunctionality

The tough gelatin eutectogels also exhibit good adhesion ability, environmental tolerance, and recyclability. As shown in

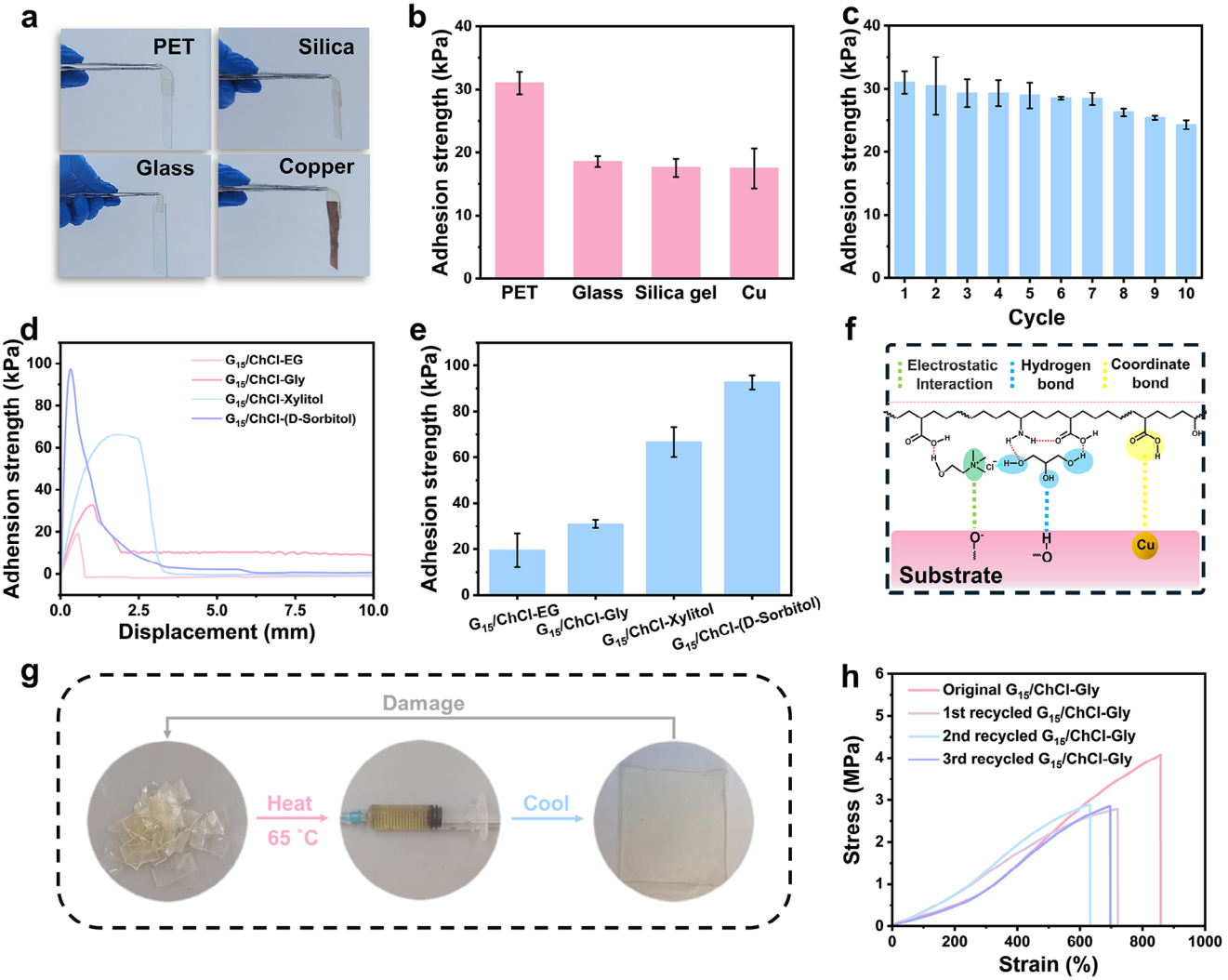

Figure 5. Adhesive and recycling properties of gelatin eutectogels. a) Photographs illustrating the adhesiveness of G_{15}/ChCl-Gly gel on different substrates (PET, Glass sheet, Silica sheet, Copper sheet). b) Adhesive strength of G_{15}/ChCl-Gly gel on various substrates. c) Ten repeated adhesion strength of G_{15}/ChCl-Gly gel on PET. d) Adhesion curves and e) the corresponding adhesion strength of different gelatin eutectogels (G_{15}/ChCl-EG, G_{15}/ChCl-Gly, G_{15}/ChCl-Xylitol, G_{15}/ChCl-(D-Sorbitol) on PET. f) Schematic adhesion mechanisms of gelatin eutectogels. g) Optical photos showing schematic diagram of the recyclability of G_{15}/ChCl-Gly gel. h) Tensile stress-strain curves of G_{15}/ChCl-Gly gel before and after recycling. Data in (b), (c), and (e) are represented as mean values ± SD ($n = 3$).

Figure 5a, the G_{15}/ChCl-Gly gel sample could tightly adhere to different substrates (including polyethylene glycol terephthalate (PET), glass sheet, silica sheet and copper sheet). The adhesive strengths of the gel to glass, PET, Cu and silica sheet substrates were quantified to be 30.98 ± 1.81, 18.53 ± 0.88, 17.56 ± 1.43, and 17.43 ± 3.15 kPa, respectively (Figure S18a, Supporting Information, Figure 5b). In addition, these reversible non-covalent interactions enable repeatable adhesion. For example, the adhesion strength to PET remained at ≈23 kPa after 10 attach and detach cycles (Figure S18b, Supporting Information, Figure 5c). Furthermore, using the PET as the typical substrate, the adhesion property of various gelatin eutectogels was quantitatively evaluated (Figure 5d,e). As the hydroxyl number in the hydrogen bond donor (HBD) increased, the adhesive strength of the prepared eutectogels also improved. This enhancement can be attributed to the higher number of hydroxyl groups, which strengthen interfacial interactions, as well as increasing toughness of the eutectogels. As a result, the adhesive performance of gelatin eutectogels can be regulated and the adhesive strength of the G_{15}/ChCl-(D-Sorbitol) gel to PET was as high as 92.64 ± 3.10 kPa. Such good adhesion could be attributed to the numerous hydrogen bonds, electrostatic interactions and metal coordination provided by carboxyl, amido and hydroxyl groups (Figure 5f).[59,60]

DESs demonstrate unique characteristics such as high ionic conductivity, low vapor pressure and low operation temperature.[61] The gelatin eutectogels have composed of such advantageous characteristics. For instance, the prepared gelatin eutectogels had varying ionic conductivity depending on the types of DESs and the density of crosslinked network (Figure S19, Supporting Information). The gelatin eutectogels also exhibited excellent low-temperature tolerance. As revealed by Differential Scanning Calorimetry (DSC) measurements (Figure S20a,

Supporting Information), different from gelatin hydrogel with a freezing point at −20.46 °C, our gelatin eutectogels remained stable within the temperature range of −70 to 20 °C. Such excellent anti-freezing ability allows the eutectogels to maintain their functionalities at extreme subzero temperatures. As shown in Figure S20b, Supporting Information, with the decrease of temperature, the G_{15}/ChCl-Gly gel gradually became stiffer, but was still highly stretchable with a strain at break of 535% at −40 °C. And the conductivity of G_{15}/ChCl-Gly gel gradually decreased as the temperature decreased, and the conductivity of it was 0.088 mS cm^{-1} at −20 °C due to the low-temperature stability (Figure S20c, Supporting Information). The G_{15}/ChCl-Gly gel also demonstrated excellent self-recovery ability at low temperature (Figure S20d,e, Supporting Information). As expected, due to the low vapor pressure of ChCl-Gly, the G_{15}/ChCl-Gly gel also exhibited long-term stability (Figure S21, Supporting Information).

The reversible non-covalent crosslinking in eutectogels endows them with good recyclability.[18] As illustrated in Figure 5g, the broken G_{15}/ChCl-Gly gel fragments can be fully transferred into a uniform sol state after heating at 65 °C by dissociating the original non-covalent bonds (hydrogen bonds and ionic interactions). The gel-to-sol transition of G_{15}/ChCl-Gly at the increased temperature was confirmed by rheological test (Figure S22, Supporting Information). After cooled back to room temperature, the non-covalent interactions between gelatin chains and ChCl-Gly were reformed, achieving the recycling of G_{15}/ChCl-Gly gel. The recycled G_{15}/ChCl-Gly gel after three recycles still retained a high tensile strain of ≈600% and a tensile strength of ≈3 MPa, although it exhibited some decrease compared with the original G_{15}/ChCl-Gly gel (Figure 5h). In addition, the recycled G_{15}/ChCl-Gly gel demonstrated higher conductivity (1.00 mS cm^{-1}) compared with that of the original ones (0.74 mS cm^{-1}) (Figure S23, Supporting Information), which attributes that the decreased crosslinked structure was conducive to ion migration. Other types of gelatin eutectogels (G_{15}/ChCl-EG, G_{15}/ChCl-Xylitol, G_{15}/ChCl-(D-Sorbitol)) also demonstrated good recyclability, as shown in Figure S24, Supporting Information. Moreover, our protein gel can degrade to basic building blocks after soaking in water for 72 h (Figure S25, Supporting Information), and the degradation ratio could reach to 94.78 ± 0.61%, suggesting their application potential in degradable surgical implants, eco-friendly soft robots and transient electronics.

2.5. Potential Applications of Gelatin Eutectogels

The strong and tough gelatin eutectogels with adjustable mechanics and multifunction (adhesiveness, ionic conductivity, and environmental stability) hold broad application potential across diverse fields under extreme environments. Due to skin-like modulus, high stretchability and toughness, the application of G_{15}/ChCl-Gly gel as flexible and wearable sensors was investigated. The strain sensing performance of G_{15}/ChCl-Gly gel was firstly evaluated (Figure S26, Supporting Information). The G_{15}/ChCl-Gly gel-based strain sensor exhibited high sensitivity with the gauge factors (GFs) of 1.59 for strain ranging from 0% to 350% and 2.45 for strain larger than 350%, respectively (Figure S26a, Supporting Information). In addition, the G_{15}/ChCl-Gly gel strain sensor demonstrated a fast response rate, with a response time of 318 ms and a recovery time of 154 ms, respectively (Figure S26b, Supporting Information). Moreover, the strain sensor can detect different levels of strain with high reliability and long-term stability (Figure S26c–h, Supporting Information). Given the outstanding strain sensitivity and sensing range, the G_{15}/ChCl-Gly gel was assembled as wearable sensors for human motions and physiological signals monitoring (Figure S27, Supporting Information). For example, the bending angles and bending speed of joints could be feasibly and accurately reflected (Figure S27a–c, Supporting Information). Apart from large joint motions, the wearable sensor can also detect slight muscle activities, such as speaking different English letters controlled by the masseter muscle and swallowing controlled by the pharyngeal muscles, with consistent and stable signals (Figure S27d,e, Supporting Information). At the same time, the wearable sensor also had a certain pressure sensing capability (Figure S27f, Supporting Information). Moreover, the excellent environmental stability of G_{15}/ChCl-Gly gel allowed the strain sensor to work at −20 °C (Figure S28, Supporting Information).

The G_{15}/ChCl-Gly gel-based bioelectrodes could be used to record trivial electrophysiological signals. A three-point detection method was used to monitor the electromyography (EMG) signals generated by muscle fibers during human movements.[21,62] The A electrode (red) and B electrode (green) based on G_{15}/ChCl-Gly gels were placed on the head and tail of biceps brachii/palmaris longus muscle as working electrode and reference electrode, respectively. The C electrode (black) was fixed on the right lower limb of volunteers as grounding electrode (Figure S29a, Supporting Information). The EMG signals were highly consistent when holding the gripper with same force. A gradual increase in signal strength was observed as the holding force varied between 5, 10, and 15 kg (Figure S29b, Supporting Information), which was comparable to the commercial Ag/AgCl electrodes (Figure S29c, Supporting Information). These results indicate that G_{15}/ChCl-Gly gel-based electrodes were highly qualified for recording EMG signals. Similarly, three G_{15}/ChCl-Gly gel-based electrodes were employed as bioelectrodes for electrocardiogram (ECG) signal acquisition. Specifically, electrodes A (red) and B (green) were placed on the left and right radial pulses as the working and reference electrodes, respectively, while electrode C (black) was attached to the volunteer's right lower limb as the ground electrode (**Figure 6a**). As shown in Figure 6b, the gel-based electrodes were able to capture ECG signals with obvious PQRST waveforms with high signal resolution and stability, which were comparable to those obtained by commercial Ag/AgCl electrodes. At the same time, we recorded ECG signals of the volunteer before and after exercise (Figure S30, Supporting Information). It can be found that the volunteers' heart rate increased from 77 to 89 bmp after the exercise. At the same time, G_{15}/ChCl-Gly gel-based electrodes also had good long-term stability for continuous ECG monitoring (Figure S31, Supporting Information). Combined with their adhesiveness, wide operation temperature range and recycling ability, G_{15}/ChCl-Gly gel-based electrodes can serve as a promising alternative to commercial Ag/AgCl electrodes.

For practical applications, the gels may need to maintain structural stability and function under great stress or strenuous movements.[63] And G_{15}/ChCl-(D-sorbitol) gel with high

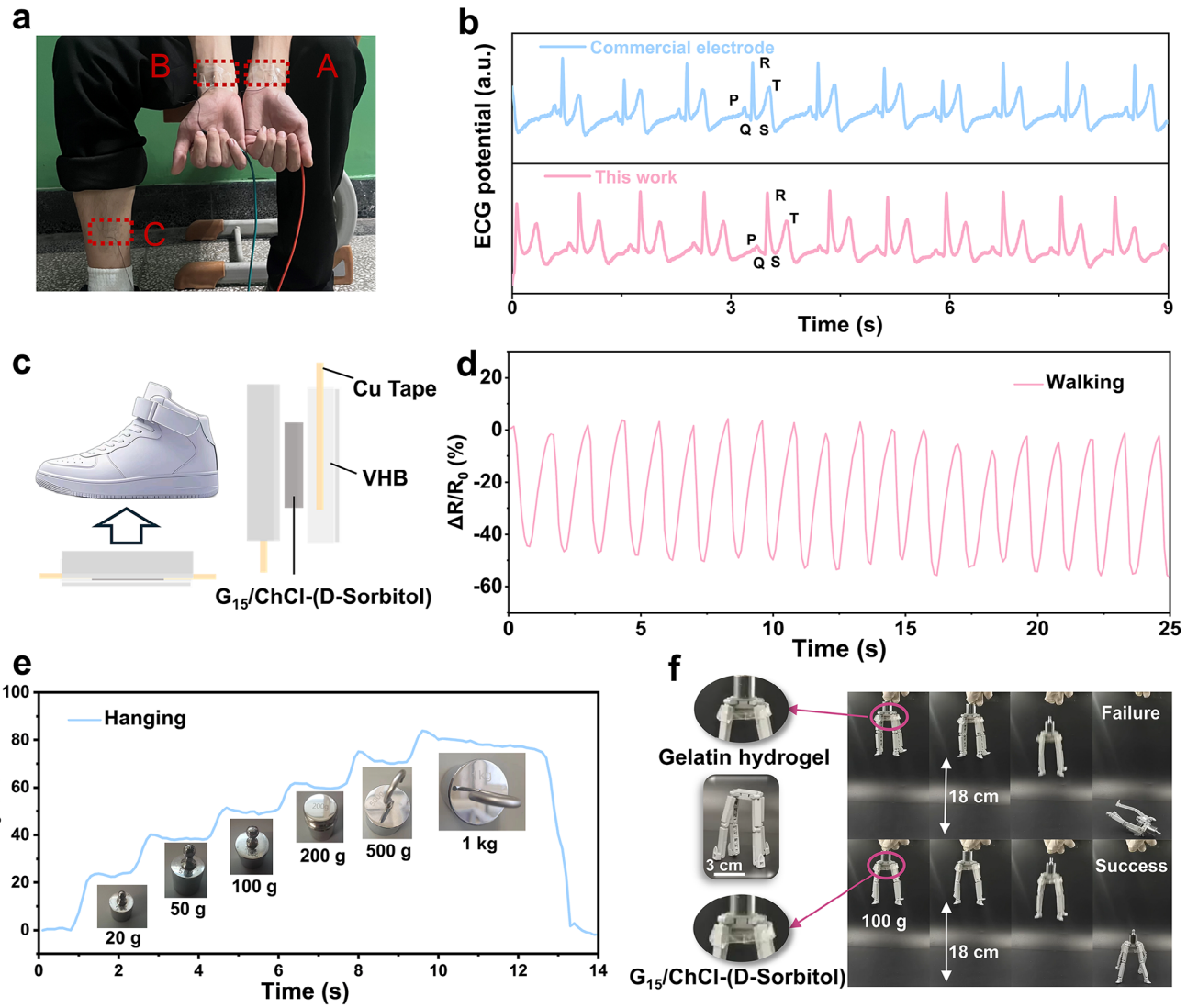

Figure 6. Demonstration of the potential application of gelatin eutectogels. a) Schematic diagram of the setup for the ECG recording (A: Working electrode, B: reference electrode, C: grounding electrode). b) ECG monitoring using G_{15}/ChCl-Gly gel electrodes and commercial Ag/AgCl gel electrodes. c) Schematic diagram of G_{15}/ChCl-(D-sorbitol) gel-based trampling sensor. d) Relative resistance changes of G_{15}/ChCl-(D-sorbitol) gel-based sensor during walking. e) Relative resistance curves of G_{15}/ChCl-(D-sorbitol) gel upon hanging objects of different weights. f) Landing conditions of lander before and after being fixed by gelatin hydrogel and G_{15}/ChCl-(D-sorbitol) gel.

stiffness, strength and toughness in our work is satisfied for applications in such conditions. As demonstrated in Figure 6c, G_{15}/ChCl-(D-sorbitol) gel was assembled and encapsulated between two VHB tapes as a strain sensor, which was placed under foot to record the walking signals. Figure 6d shows that the clear and stable sensing signals can be obtained during working. Similarly, we hung weights of varying magnitudes on the G_{15}/ChCl-(D-sorbitol) gel (20 mm × 10 mm × 0.4 mm) to detect the resistance signal of the gel under the tension of different weights. The G_{15}/ChCl-(D-sorbitol) gel can bear the weights from 20 g to 1 kg and output a stable resistance signal (Figure 6e). Furthermore, the applications of strong and tough gelatin eutectogels as load-bearing materials was demonstrated by using G_{15}/ChCl-(D-sorbitol) gel as the load-bearing belt of the landing leg of a soft lander (Figure 6f).[64] This lander has four articulated legs that can be opened and closed freely. Four eutectogel strips (40 mm × 10 mm × 0.4 mm) link the four legs through the adhesive connection of the gel itself, so that they are subjected to static or vertical impact loads when the lander is in the ground. The lander with a weight of 100 g without gel (the total weight of 117 g) was lifted to a height of 18 cm, and then was released for free fall. The function of energy absorbed by the instantaneous elongation of gel connected to the lander is similar to that of tendons. As a comparison, the lander with gelatin hydrogel as load-bearing belt cannot withstand the impact during landing due to the weak mechanical strength. While, after being reinforced with G_{15}/ChCl-(D-sorbitol) gel, the lander can withstand impact and land stably in free fall, demonstrating its potential applications as load-bearing materials in soft devices.

3. Conclusion

In summary, we developed strong, stiff, tough and durable protein gels based on gelatin (named as gelatin eutectogels) using DESs as dispersion medium with feasible solvent-exchange strategy. By replacing water with DES solvent, the gelatin chain–chain interaction was greatly enhanced, and DESs formed numerous non-covalent crosslinks among gelatin chains, enabling gelatin eutectogels with high strength, high stiffness, excellent toughness, superior stretchability and crack-insensitivity. Moreover, the mechanical performance of gelatin eutectogels can be customized by adopting different polyols as HBDs to regulate the hydrogen bonds between DESs and gelatin chains. In addition, such reversible crosslinking structure featured the gelatin eutectogels with multi-functionalities, including adhesiveness, recyclability, anti-freezing properties, and degradation. The potential application of these versatile and robust gelatin eutectogels was preliminarily demonstrated in wearable sensors capable of detecting subtle or intense biological activities and load-bearing parts within soft robotic systems. This work provides a feasible route to prepare a tough, strong, and stiff protein-based gel with multi-functions, which paves the way for the integration of protein gels into technologies demanding customizable mechanical and structural features.

Supporting Information

Supporting Information is available from the Wiley Online Library or from the author.

Acknowledgements

The authors greatly appreciate the financial support of the National Natural Science Foundation of China (Nos. 22102139, 22372143 and 22072127) and the Hebei Natural Science Foundation (Nos. B2021203001, B2025203022 and B2021203016).

Conflict of Interest

The authors declare no conflict of interest.

Data Availability Statement

The data that support the findings of this study are available from the corresponding author upon reasonable request.

Keywords

fracture resistance, hydrogen bond donor, protein gel, solvent-toughening, strong and tough

Received: April 7, 2025
Revised: June 3, 2025
Published online:

[1] L. Fu, L. Li, Q. Bian, B. Xue, J. Jin, J. Li, Y. Cao, Q. Jiang, H. Li, *Nature* **2023**, *618*, 740.
[2] D. Lin, M. Li, L. Wang, J. Cheng, Y. Yang, H. Wang, J. Ye, Y. Liu, *Adv. Funct. Mater.* **2024**, *34*, 2405255.
[3] Z. Leng, P. Zhu, X. Wang, Y. Wang, P. Li, W. Huang, B. Li, R. Jin, N. Han, J. Wu, *Adv. Funct. Mater.* **2023**, *33*, 2211056.
[4] S. Gomes, I. B. Leonor, J. F. Mano, R. L. Reis, D. L. Kaplan, *Prog. Polym. Sci.* **2012**, *37*, 1.
[5] J. Wu, J. H. Lei, M. Li, A. Zhang, Y. Li, X. Liang, S. C. de Souza, Z. Yuan, C. Wang, G. Chen, *Adv. Sci.* **2024**, *11*, 2404702.
[6] C. Wang, T. Yokota, T. Someya, *Chem. Rev.* **2021**, *121*, 2109.
[7] X. Yuan, W. Kong, P. Xia, Z. Wang, Q. Gao, J. Xu, D. Shan, Q. Yao, Z. Ma, B. Guo, *Adv. Funct. Mater.* **2024**, *34*, 2404824.
[8] M. Baumgartner, F. Hartmann, M. Drack, D. Preninger, D. Wirthl, R. Gerstmayr, L. Lehner, G. Mao, R. Pruckner, S. Demchyshyn, *Nat. Mater.* **2020**, *19*, 1102.
[9] T. Ji, H. Shi, X. Yang, H. Li, D. L. Kaplan, J. Yeo, W. Huang, *Adv. Healthcare Mater.* **2024**, *13*, 2401562.
[10] X. Zhao, X. Chen, H. Yuk, S. Lin, X. Liu, G. Parada, *Chem. Rev.* **2021**, *121*, 4309.
[11] Z. Wang, X. Song, X. Li, X. Yue, S. Hou, L. Liu, *Chem. Mater.* **2022**, *34*, 10917.
[12] M. Mihajlovic, M. Staropoli, M. S. Appavou, H. M. Wyss, W. Pyckhout-Hintzen, R. P. Sijbesma, *Macromolecules* **2017**, *50*, 3333.
[13] X. Hou, B. Huang, L. Zhou, S. Liu, J. Kong, C. He, *Adv. Mater.* **2023**, *35*, 2301532.
[14] X. Li, J. P. Gong, *Proc. Natl. Acad. Sci. U. S. A.* **2022**, *119*, 2200678119.
[15] X. Hu, M. Vatankhah-Varnoosfaderani, J. Zhou, Q. Li, *Adv. Mater.* **2015**, *27*, 6899.
[16] X. N. Zhang, Y. J. Wang, S. Sun, L. Hou, P. Wu, Z. L. Wu, Q. Zheng, *Macromolecules* **2018**, *51*, 8136.
[17] M. A. Gonzalez, J. R. Simon, A. Ghoorchian, Z. Scholl, S. Lin, M. Rubinstein, P. Marszalek, A. Chilkoti, G. P. López, X. Zhao, *Adv. Mater.* **2017**, *29*, 1604743.
[18] Z. Qin, X. Sun, H. Zhang, Q. Yu, X. Wang, S. He, F. Yao, J. Li, *J. Mater. Chem. A* **2020**, *8*, 4447.
[19] X. Yuan, Z. Zhu, P. Xia, Z. Wang, X. Zhao, X. Jiang, T. Wang, Q. Gao, J. Xu, D. Shan, *Adv. Sci.* **2023**, *10*, 2301665.
[20] Q. He, Y. Huang, S. Wang, *Adv. Funct. Mater.* **2018**, *28*, 1705069.
[21] L. Lan, J. Ping, H. Li, C. Wang, G. Li, J. Song, Y. Ying, *Adv. Mater.* **2024**, *36*, 2401151.
[22] Y. Shen, A. Levin, A. Kamada, Z. Toprakcioglu, M. Rodriguez-Garcia, Y. Xu, T. P. Knowles, *ACS Nano* **2021**, *15*, 5819.
[23] X. Sun, Y. Mao, Z. Yu, P. Yang, F. Jiang, *Adv. Mater.* **2024**, *26*, 2400084.
[24] M. Wang, X. Xiao, S. Siddika, M. Shamsi, E. Frey, W. Qian, W. Bai, B. T. O'Connor, M. D. Dickey, *Nature* **2024**, *631*, 313.
[25] B. B. Hansen, S. Spittle, B. Chen, D. Poe, Y. Zhang, J. M. Klein, A. Horton, L. Adhikari, T. Zelovich, B. W. Doherty, *Chem. Rev.* **2020**, *121*, 1232.
[26] M. Criado-Gonzalez, N. Alegret, A. M. Fracaroli, D. Mantione, G. Guzmán-González, G. Del Olmo, D. Mecerreyes, *Angew. Chem.* **2023**, *135*, 202301489.
[27] H. Qin, R. E. Owyeung, S. R. Sonkusale, M. J. Panzer, *J. Mater. Chem. C* **2019**, *7*, 601.
[28] S. Wei, J. Xu, W. Zhao, X. Li, W. Zhao, S. Yan, *Adv. Funct. Mater.* **2024**, *34*, 2408648.
[29] M. L. Picchio, M. S. Orellano, M. A. Motta, C. Huck-Iriart, D. Sánchez-deAlcázar, R. López-Domene, B. Martín-García, A. Larrañaga, A. Beloqui, D. Mecerreyes, *Adv. Funct. Mater.* **2024**, *34*, 2313747.
[30] L. Weng, M. Toner, *Phys. Chem. Chem. Phys.* **2018**, *20*, 22455.
[31] R. Liu, C. Qiao, Q. Liu, L. Liu, J. Yao, *ACS Appl. Polym. Mater.* **2023**, *5*, 4546.
[32] X. Zhang, Z. Zhang, T. Zhang, Y. Zhang, L. Jiang, X. Sui, *Food Hydrocolloids* **2025**, *158*, 110533.
[33] K. Zong, K. Li, Z. Zhou, L. Gong, D. Deng, *New J. Chem.* **2022**, *46*, 15959.

[34] I. Székely-Szentmiklósi, E. M. Rédai, Z.-I. Szabó, B. Kovács, C. Albert, A.-L. Gergely, B. Székely-Szentmiklósi, E. Sipos, *Foods* **2024**, *13*, 2935.
[35] A. Kjar, M. R. Haschert, J. C. Zepeda, A. J. Simmons, A. Yates, D. Chavarria, M. Fernandez, G. Robertson, A. M. Abdulrahman, H. Kim, *Cell Rep.* **2024**, *43*, 114874.
[36] P. Liu, C. M. Pedersen, J. Zhang, R. Liu, Z. Zhang, X. Hou, Y. Wang, *Green Energy Environ.* **2021**, *6*, 261.
[37] J. Kumankuma-Sarpong, C. Chang, J. Hao, T. Li, X. Deng, C. Han, B. Li, *Adv. Mater.* **2024**, *36*, 2403214.
[38] C. Qiao, X. Ma, J. Zhang, J. Yao, *Food Chem.* **2017**, *235*, 45.
[39] F. A. Whitehead, S. A. Young, S. Kasapis, *Int. J. Biol. Macromol.* **2019**, *141*, 867.
[40] K. Hofstetter, B. Hinterstoisser, L. Salmén, *Cellulose* **2006**, *13*, 131.
[41] Y. Li, D. Wang, J. Wen, J. Liu, D. Zhang, J. Li, H. Chu, *Adv. Funct. Mater.* **2021**, *31*, 2011259.
[42] H. Wang, H. Liu, Z. Cao, W. Li, X. Huang, Y. Zhu, F. Ling, H. Xu, Q. Wu, Y. Peng, *Proc. Natl. Acad. Sci. U. S. A.* **2020**, *117*, 11299.
[43] J. Wang, B. Wu, P. Wei, S. Sun, P. Wu, *Nat. Commun.* **2022**, *13*, 4411.
[44] L. Meng, Y. Hu, W. Li, Z. Zhou, S. Cui, M. Wang, Z. Chen, Q. Wu, *ACS Appl. Mater. Interfaces* **2024**, *16*, 53007.
[45] E. I. Wisotzki, P. Tempesti, E. Fratini, S. G. Mayr, *Phys. Chem. Chem. Phys.* **2017**, *19*, 12064.
[46] T. Kämäräinen, S. Nogami, H. Arima-Osonoi, H. Iwase, H. Uchiyama, Y. Tozuka, K. Kadota, *J. Colloid Interface Sci.* **2024**, *669*, 975.
[47] Y. Yang, X. Wang, F. Yang, L. Wang, D. Wu, *Adv. Mater.* **2018**, *30*, 1707071.
[48] L. B. Jiang, D. H. Su, S. L. Ding, Q. C. Zhang, Z. F. Li, F. C. Chen, W. Ding, S. T. Zhang, J. Dong, *Adv. Funct. Mater.* **2019**, *29*, 1901314.
[49] J. Wu, P. Li, C. Dong, H. Jiang, B. Xue, X. Gao, Y. Cao, *Nat. Commun.* **2018**, *9*, 620.
[50] J. Fang, A. Mehlich, N. Koga, J. Huang, R. Koga, X. Gao, C. Hu, C. Jin, M. Rief, J. Kast, *Nat. Commun.* **2013**, *4*, 2974.
[51] Z. Li, Z. Zheng, Y. Yang, G. Fang, J. Yao, Z. Shao, X. Chen, *ACS Sustainable Chem. Eng.* **2016**, *4*, 1500.
[52] D. Zhou, F. Chen, J. Wang, T. Li, B. Li, J. Zhang, X. Zhou, T. Gan, S. Handschuh-Wang, X. Zhou, *J. Mater. Chem. B.* **2018**, *6*, 7366.
[53] Y. Fu, Q. Lin, R. Lan, Z. Shao, *Small* **2024**, *20*, 2403376.
[54] T. Lan, Y. Dong, J. Shi, X. Wang, Z. Xu, Y. Zhang, L. Jiang, W. Zhou, X. Sui, *Aggregate* **2024**, *5*, 639.
[55] X. Zhang, L. Xiao, Z. Ding, Q. Lu, D. L. Kaplan, *ACS Nano* **2022**, *16*, 10209.
[56] L. Xu, C. Wang, Y. Cui, A. Li, Y. Qiao, D. Qiu, *Sci. Adv.* **2019**, *5*, 3442.
[57] L. Li, W. Li, X. Wang, X. Zou, S. Zheng, Z. Liu, Q. Li, Q. Xia, F. Yan, *Angew. Chem.* **2022**,.*134*, 202212512.
[58] J. Xiong, M. Duan, X. Zou, S. Gao, J. Guo, X. Wang, Q. Li, W. Li, X. Wang, F. Yan, *J. Am. Chem. Soc.* **2024**, *146*, 13903.
[59] H. Wang, M. Wang, J. Wu, S. Zhu, Y. Ye, Y. Liu, K. Li, R. Li, Y. Zhang, M. Wei, *Adv. Healthcare Mater.* **2024**, *13*, 2304444.
[60] X. Liu, Q. Zhang, Z. Gao, R. Hou, G. Gao, *ACS Appl. Mater. Interfaces* **2017**, *9*, 17645.
[61] Y. Zhang, Y. Wang, Y. Guan, Y. Zhang, *Nat. Commun.* **2022**, *13*, 6671.
[62] Y. Liu, C. Wang, J. Xue, G. Huang, S. Zheng, K. Zhao, J. Huang, Y. Wang, Y. Zhang, T. Yin, *Adv. Healthcare Mater.* **2022**, *11*, 2200653.
[63] X. Fan, Y. Luo, K. Li, Y. J. Wong, C. Wang, J. C. C. Yeo, G. Yang, J. Li, X. J. Loh, Z. Li, *Adv. Mater.* **2024**, *36*, 2407398.
[64] Y. H. Fang, C. Liang, V. Liljeström, Z. P. Lv, O. Ikkala, H. Zhang, *Adv. Mater.* **2024**, *36*, 2402282.